Multigrid–Based Optimal Shape and Topology Design in Magnetostatics*

Dalibor Lukáš[1]

Department of Applied Mathematics, VŠB–Technical University of Ostrava,
17. listopadu 15, 708 33 Ostrava–Poruba, Czech Republic

Abstract. The paper deals with an efficient solution technique to large–scale discretized shape and topology optimization problems. The efficiency relies on multigrid preconditioning. In case of shape optimization, we apply a geometric multigrid preconditioner to eliminate the underlying state equation while the outer optimization loop is the sequential quadratic programming, which is done in the multilevel fashion as well. In case of topology optimization, we can only use the steepest–descent optimization method, since the topology Hessian is dense and large–scale. We also discuss a Newton–Lagrange technique, which leads to a sequential solution of large–scale, but sparse saddle–point systems, that are solved by an augmented Lagrangian method with a multigrid preconditioning. At the end, we present a sequential coupling of the topology and shape optimization. Numerical results are given for a geometry optimization in 2–dimensional nonlinear magnetostatics.

1 Introduction

The process of engineering design involves proposing a new prototype, testing it and improvements towards another prototype. This loop can be simulated on a computer if we can exactly determine the design space of improvements, the objective function which evaluates the tests, and the state constraints that model the underlying physical laws. Nowadays, with the rapid progress in computing facilities, the computer aided design requires software tools that are able to solve problems which still fit to the memory (milions of unknowns) and their solution times are in terms of hours. In this spirit, multigrid techniques [2, 7] proved to be the relevant methods for partial differential equations. Recently, they have been extended to multigrid–based optimization in optimal control [1, 11], in parameter identification [4] or in topology optimization [6]. This paper is a summary of our recent contributions within the multigrid optimization context [8, 9]. Moreover, it extends our latest development in multigrid preconditioning of mixed systems [10] towards the topology optimization.

* This research has been supported by the Czech Ministry of Education under the grant AVČR 1ET400300415, by the Czech Grant Agency under the grant GAČR 201/05/P008 and by the Austrian Science Fund FWF within the SFB "Numerical and Symbolic Scientific Computing" under the grant SFB F013, subproject F1309.

We consider a sufficiently regular fixed computational domain $\Omega \in \mathbb{R}^2$ and the weak formulation of the following 2–dimensional nonlinear magnetostatical state problem:

$$\begin{cases} -\mathrm{div}\left(\nu(x, \|\mathrm{grad}(u(x))\|^2, q(x))\,\mathrm{grad}(u(x))\right) = J(x) & \text{for x} \in \Omega, \\ u(x) = 0 & \text{for x} \in \partial\Omega, \end{cases} \tag{1}$$

where u denotes a scalar magnetic potential so that $\mathrm{curl}(u) := (\partial u/\partial x_2, -\partial u/\partial x_1)$ is a magnetic flux density, J denotes an electric current density and ν is the following nonlinear magnetic reluctivity:

$$\nu(x, \eta, q(x)) := \nu_0 + (\nu(\eta) - \nu_0)q(x), \quad \nu(\eta) := \nu_1 + (\nu_0 - \nu_1)\frac{\eta^4}{\eta^4 + \nu_0^{-1}},$$

where $\nu_0 := 1/(4\pi 10^{-7})$ [mH^{-1}], $\nu_1 := 5100\,\nu_0$ is the air and ferromagnetic reluctivity, respectively, and where $q : \Omega \to \{0, 1\}$ denotes a topology design, which tells us whether the point x belongs to the air or the ferromagnetics.

As a typical example we consider a direct electric current (DC) electromagnet, see Fig. 1. It is used for measurements of Kerr magnetooptic effects with

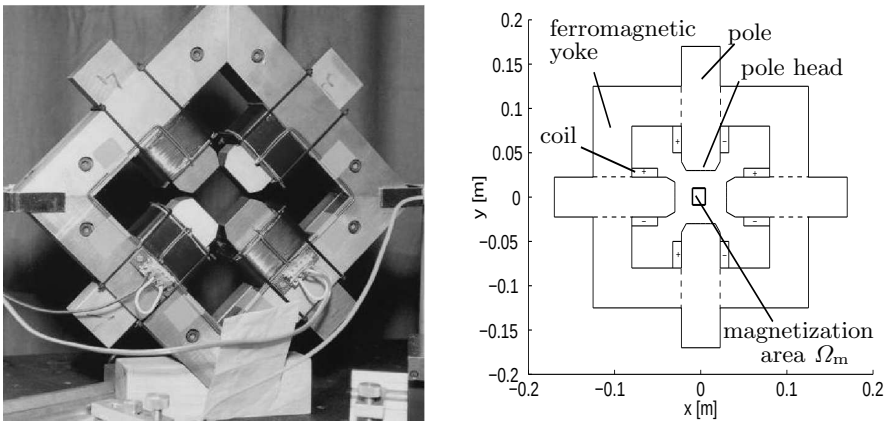

Fig. 1. Benchmark problem

applications in development of high–density magnetic or optic data recording media. The measurements require the magnetic field among the pole heads to match a prescribed constant field. Our aim is to design a geometry of the ferromagnetic yoke and pole heads that preserves the requirement. We will discuss topology optimization, where only the current sources are fixed, as well as shape optimization, where, additionally, some initial topology is fixed, which makes the computation less expensive due to the less freedom in the design.

In the shape optimization case, we fix the topology, which means that the shape design splits the domain Ω into two distinct subdomains as follows:

$$q(x,p) := \begin{cases} 0 \text{ for x} \in \Omega_0(\text{p}), \\ 1 \text{ for x} \in \Omega_1(\text{p}), \end{cases}$$

where $p \in \mathcal{P}$ denotes a parametrization, e.g. Béziér, of the shape of the splitting interface $\Gamma(p) := \partial\Omega_0(p) \cap \partial\Omega_1(p)$. Then, we consider the following shape optimization problem:

$$\begin{cases} \min\limits_{p \in P} \mathcal{I}(u(p)) \\ \text{subject to (1) and } |\Omega_1(\text{p})| \leq \text{V}_{\max}, \end{cases} \tag{2}$$

where $V_{\max} > 0$ denotes a maximal admissible volume of the ferromagnetic parts. We assume $\mathcal{I}$ to be twice differentiable and coercive and $\mathcal{P}$ to be a compact set of sufficiently regular shapes. In our experiments $\mathcal{I}$ will measure inhomogeneities of the magnetic field density in the following manner:

$$\mathcal{I}(u) := \frac{1}{2|\Omega_{\text{m}}|} \int_{\Omega_{\text{m}}} \|\text{curl}(u(x)) - B_{\text{given}}\|^2 \, dx + \frac{\varepsilon_u}{2|\Omega|} \int_{\Omega} \|\nabla u\|^2 \, dx,$$

where the term with $\varepsilon_u > 0$ regularizes the coercitivity and Ω_{m} is as in Fig. 1.

In the topology optimization case, we relax the integer constraint $q(x) \in \{0,1\}$ to the continuous constraint $q \in [0,1]$ so that in (1) we replace $q(x)$ by $q_\rho(q(x))$, which is the following penalization of intermediate values:

$$q_\rho(q) := \frac{1}{2}\left(1 + \frac{1}{\arctan(\rho)} \arctan(\rho(2q-1))\right)$$

with $\rho \gg 0$ being the penalty parameter. The relevant topology optimization problem under consideration reads as follows:

$$\begin{cases} \min\limits_{q \in Q} \left\{ \mathcal{I}(u(q_\rho(q))) + \frac{\varepsilon_q}{2|\Omega|} \int_\Omega q^2 \, dx \right\} \\ \text{subject to (1) and } \int_\Omega q_\rho(q(x)) \, dx \leq V_{\max}, \end{cases} \tag{3}$$

where $Q := \left\{ q \in L^2(\Omega) : 0 \leq q \leq 1 \right\}$ and the additional term in the objective functional, with $\varepsilon_q > 0$, regularizes its coercitivity with respect to q.

2 Multigrid Nested Shape and Topology Optimization

We aim at an efficient numerical solution to large–scale discretized shape optimization problems arising from (2). In this case the number of design variables is one–order less than the number of state variables, thus the shape Hessian is dense, but rather small, and the overall computational work is performed in the state elimination. After a discretization, the state equation (1) leads to the following nonlinear system of equations:

$$\mathbf{A}(\mathbf{u}, \mathbf{q}(\mathbf{p}))\mathbf{u} = \mathbf{J}.$$

The latter is solved by the nested approach, which means that $\mathbf{u}$ in the equation above is eliminated for each shape design $\mathbf{p}$ using a nested Newton method with multigrid preconditioned conjugate gradients (MCG) method in the most inner iterations. We propose to couple this nested Newton method with the most outer quasi–Newton optimization method as depicted in Fig. 2.

Given $\mathbf{p}_{\text{init}}$, discretize at the first level: $h^{(1)} \longrightarrow \mathbf{p}_{\text{init}}^{(1)}, \mathbf{A}^{(1)}, \mathbf{J}^{(1)}$.
Solve by a quasi-Newton method coupled with a nested Newton method, while using a nested direct solver: $\mathbf{p}_{\text{init}}^{(1)} \longrightarrow \mathbf{p}_{\text{opt}}^{(1)}$.
Store the first level preconditioner $\mathbf{C}^{(1)} := \left[\mathbf{A}_{\text{lin}}^{(1)}(\mathbf{p}_{\text{opt}}^{(1)})\right]^{-1}$.
FOR $l = 2, \ldots$ DO
  Refine: $h^{(l-1)} \longrightarrow h^{(l)}, \mathbf{p}_{\text{init}}^{(l)}, \mathbf{A}^{(l)}, \mathbf{J}^{(l)}$.
  Prolong: $\mathbf{p}_{\text{opt}}^{(l-1)} \longrightarrow \mathbf{p}_{\text{init}}^{(l)}$.
  Solve by a quasi-Newton method coupled with a nested Newton method, while using the nested MCG method preconditioned with $\mathbf{C}^{(l-1)}$: $\mathbf{p}_{\text{init}}^{(l)} \longrightarrow \mathbf{p}_{\text{opt}}^{(l)}$.
  Store the l–th level multigrid preconditioner $\mathbf{C}^{(l)} \approx \left[\mathbf{A}_{\text{lin}}^{(l)}(\mathbf{p}_{\text{opt}}^{(l)})\right]^{-1}$.
END FOR

Fig. 2. Multigrid shape optimization: the algorithm

For numerical experiments, which were computed using the software Netgen/NgSolve developed by Joachim Schöberl et al. at the University Linz, Austria, see Tab. 2. In the table the second and the fourth column respectively depict the numbers of shape design variables and the numbers of nodes in the discretizations. We can observe an optimal behaviour in terms of the CG iterations, see the numbers before the slash in the sixth column, that are preconditioned using the same geometric multigrid preconditioner throughout the whole algorithm, thus it effectively acts for changing designs $\mathbf{p}$. The multigrid preconditioner is built from the linearizations $\mathbf{A}_{\text{lin}}^{(l)}(\mathbf{p}_{\text{opt}}^{(l)}) := \mathrm{d}\mathbf{A}^{(l)}(\mathbf{0}, \mathbf{p}_{\text{opt}}^{(l)})/\mathrm{d}\mathbf{u}$, therefore, the numbers of iterations within the nonlinear steps decay, see the numbers after the slash in the sixth column. Note also that the sensitivity analysis for the shape optimization is performed via an adjoint nonlinear equation, the solution of which takes about the same computational work as the nested state elimination Newton method, which we have to differentiate in the usual adjoint sense, see [9] for the details.

In case of nested topology optimization we avoid a Newton technique in the outer optimization loop, as the topology Hessian is both dense and large–scale. Therefore, we use a steepest–descent optimization method. With this only difference we can apply the algorithm from Fig. 2 to the problem (3). The topology sensitivity analysis is again as expensive as the cost evaluation, when using the adjoint method.

level	design variables	outer iterations	state variables	maximal inner iterations	CG steps linear/nonlinear	time
1	19	10	1098	3	direct solver	32s
2	40	15	4240	3	**3**/14–25	2min 52s
3	82	9	16659	4	**4–5**/9–48	9min 3s
4	166	10	66037	4	**4–6**/13–88	49min 29s
5	334	13	262953	5	**3–6**/20–80	6h 36min

Table 1. Multigrid shape optimization: numerical results

3 Multigrid All–at–Once Topology Optimization

Now we aim at developing a Newton method for large–scale discretized topology optimization problems arising from (3). For sake of clarity, let us assume the ferromagnetic reluctivity to be constant $\nu(\eta) := \nu_1$, which is the case of linear magnetostatics. Contrary to shape optimization, in topology optimization the numbers of state and design variables are of the same order, therefore the topology Hessian is both dense and large–scale, and the nested Newton approach can not be applied. We rather prescribe the state constraint in terms of a Lagrange multiplier $\lambda \in H_0^1(\Omega)$ and we propose to use an active set strategy to fulfill the other inequality constraints. This leads to a sequence of the following saddle–point systems, which are large–scale, but sparse and well–structured: Find $(\delta u_k, \delta q_k, \delta\lambda_k) \in H_0^1(\Omega) \times L^2(\Omega) \times H_0^1(\Omega)$:

$$\begin{pmatrix} L & , & \text{sym.} & , \text{sym.} \\ B(\lambda_k, q_k) & , & I(u_k, q_k, \lambda_k) & , \text{sym.} \\ L(q_k) & , & B(u_k, q_k)^T & , \quad 0 \end{pmatrix} \begin{pmatrix} \delta u_k \\ \delta q_k \\ \delta\lambda_k \end{pmatrix} = - \begin{pmatrix} f(u_k, q_k, \lambda_k) \\ g(u_k, q_k, \lambda_k) \\ c(u_k, q_k) \end{pmatrix} \tag{4}$$

where the entries are the following bilinear or linear forms:

$$L(u,v) := \int_\Omega (1|_{\Omega_\mathrm{m}} + \varepsilon_u)\nabla u \nabla v \, dx, \quad L(q_k)(u,v) := \int_\Omega \nu(q_\rho(q_k))\nabla u \nabla v \, dx,$$

$$B(v_k, q_k)(p,v) := \int_\Omega (\nu_1 - \nu_0)\frac{\mathrm{d}\, q_\rho}{\mathrm{d}\, q}(q_k)\nabla v_k p \nabla v \, dx,$$

$$I(u_k, q_k, \lambda_k)(p,q) := \int_\Omega \left(\varepsilon_q + (\nu_1 - \nu_0)\frac{\mathrm{d}^2\, q_\rho}{\mathrm{d}\, q^2}(q_k)\nabla u_k \nabla \lambda_k\right) p\, q \, dx,$$

$$f(u_k, q_k, \lambda_k)(v) := \int_{\Omega_\mathrm{m}} (\mathrm{curl}(u_k) - B_\mathrm{given})\,\mathrm{curl}(v)\, dx$$

$$+ \int_\Omega (\varepsilon_u \nabla u_k + \nu(q_\rho(q_k))\nabla\lambda_k)\,\nabla v \, dx,$$

$$g(u_k, q_k, \lambda_k)(p) := \int_\Omega \left(\varepsilon_q q_k + (\nu_1 - \nu_0)\frac{\mathrm{d}\, q_\rho}{\mathrm{d}\, q}(q_k)\nabla u_k \nabla \lambda_k\right) p \, dx,$$

$$c(u_k, q_k)(v) := \int_\Omega \nu(q_\rho(q_k))\nabla u_k \nabla v \, dx - \int_\Omega J \, v \, dx,$$

where $u, v \in H_0^1(\Omega)$, $p, q \in Q$. The update can be given by the following line–search:

$$u_{k+1} := u_k + t_k \, \delta u_k, \quad q_{k+1} := P_{\widetilde{Q}}(q_k + t_k \, \delta q_k), \quad \lambda_{k+1} := \lambda_k + t_k \, \delta \lambda_k,$$

where $t_k > 0$ and $P_{\widetilde{Q}} : L^2(\Omega) \to \widetilde{Q}$ is the projection onto $\widetilde{Q} := \{q \in Q : \int_\Omega q_\rho(q(x)) \, dx \leq V_{\max}\}$. Unfortunately, so far we have not found a successful globalization strategy to find a proper t_k, while the simple one based on minimization of the norm of the right–hand side of (4) failed.

3.1 Multigrid–Lagrange Method for the Stokes Problem

As a first step towards solution to (4), we focuse on solution to a linear system. We realize that (4) is rather similar to the 2–dimensional Stokes problem: Find $(u, q) \in [H_0^1(\Omega)]^2 \times L^2(\Omega)$:

$$\begin{pmatrix} A & , \text{sym.} \\ B & , \quad 0 \end{pmatrix} \begin{pmatrix} u \\ q \end{pmatrix} = \begin{pmatrix} F \\ 0 \end{pmatrix} \tag{5}$$

where for $v, w \in [H_0^1(\Omega)]^2$ and for $p \in L^2(\Omega)$ the operators reads as follows: $A(v, w) := \int_\Omega \sum_{i=1}^2 \nabla v_i \nabla w_i \, dx$, $B(v, p) := \int_\Omega \operatorname{div}(v) \, p \, dx$ and $F(v) := \int_\Omega f \, v \, dx$, where $f \in [L^2(\Omega)]^2$. Note that the solution is unique up to a constant hydrostatical pressure q.

Our algorithmic development is based on a variant of the augmented Lagrangian method proposed in [5], the convergence of which was proven to depend only on the smallest eigenvalue of A. Therefore, we build a multigrid preconditioner to A, denoted by $\widehat{A}^{-1}$ and the multigrid preconditioner to the $L^2(\Omega)$–inner product, denoted by $\widehat{M}^{-1}$, which leads to a method of linear computational complexity, see [10] for details. Denote the augmented Lagrange functional of (5) by

$$\mathcal{L}(u, q, \rho) := \frac{1}{2} A(u, u) - F(u) + B(q, u) + \frac{\rho}{2} \|Bu\|^2_{L^2(\Omega)'},$$

where $\|.\|_{L^2(\Omega)'}$ denotes the norm in the dual space to $L^2(\Omega)$, which can be evaluated due to the Riesz theorem as follows: $\|Bu\|_{L^2(\Omega)'} \approx \|Bu\|_{\widehat{M}^{-1}} := \sqrt{(Bu)^T \widehat{M}^{-1} (Bu)}$, where $\widehat{M}$ is an approximation of the mass matrix. The algorithm based on a semi–monotonic augmented Lagrangian technique and multigrid preconditioning is described in Fig. 3. In the algorithm the inner minimization is realized via the conjugate gradients method preconditioned with $\widehat{A}^{-1}$, i.e. the inner loop is optimal. It is important that the inner loop is terminated with a precision proportional to the violence of the constraint $Bu = 0$. From the theory in [5] and the fact that we use optimal preconditioners, it follows that also the number of outer iterations is bounded by a constant independently from the

fineness of discretization, i.e. the algorithm is of assymptoticaly linear complexity with respect to the number of unknowns. The key point for the optimality of the outer loop is that we preserve a kind of monotonicity of the augmented Lagrange functional, see Fig 3 for the condition for the increase of the penalty ρ. Under this condition we have also proven [10] a uniform upper bound on ρ.

Given $\eta > 0$, $\beta > 1$, $\nu > 0$, $\rho^{(0)} > 0$, $u^{(0)} \in V$, $p^{(0)} \in Z$, precision $\varepsilon > 0$
and feasibility precision $\varepsilon_{\text{feas}} > 0$
FOR $k := 0, 1, 2, \ldots$ DO
  Find $u^{(k+1)} : \|\nabla_u \mathcal{L}(u^{(k+1)}, p^{(k)}, \rho^{(k)})\|_{\widehat{A}^{-1}} \leq \min\left\{\nu \|Bu^{(k+1)}\|_{\widehat{M}^{-1}}, \eta\right\}$
  IF $\|\nabla_u \mathcal{L}(u^{(k+1)}, p^{(k)}, \rho^{(k)})\|_{\widehat{A}^{-1}} \leq \varepsilon$ and $\|Bu^{(k+1)}\|_{\widehat{M}^{-1}} \leq \varepsilon_{\text{feas}}$
    BREAK
  END IF
  $p^{(k+1)} := p^{(k)} + \rho^{(k)} \widehat{M}^{-1} B u^{(k+1)}$
  IF $k > 0$ and $\mathcal{L}(u^{(k+1)}, p^{(k+1)}, \rho^{(k)}) < \mathcal{L}(u^{(k)}, p^{(k)}, \rho^{(k-1)}) + \frac{\rho^{(k)}}{2} \|Bu^{(k+1)}\|^2_{\widehat{M}^{-1}}$
    $\rho^{(k+1)} := \beta \rho^{(k)}$
  ELSE
    $\rho^{(k+1)} := \rho^{(k)}$
  END IF
END FOR
$u^{(k+1)}$ is the solution.

Fig. 3. Multigrid preconditioned semi–monotonic augmented Lagrangian method

There is an advantage to the classical inexact Uzawa method [3], since in our algorithm we do not need to have independent constraints, i.e. B does not need to be a full rank matrix. Nevertheless, in case of B being full rank and with a special setup ($\beta\nu^2 \approx \rho^{(0)}$), the penalty ρ is never updated and the algorithm in Fig. 3 becomes the inexact Uzawa method applied to the system

$$\begin{pmatrix} A + \rho^{(0)} B^T \widehat{M}^{-1} B & , \text{sym.} \\ B & , \quad 0 \end{pmatrix} \begin{pmatrix} u \\ q \end{pmatrix} = \begin{pmatrix} F \\ 0 \end{pmatrix}$$

with $(1/2)\widehat{A}^{-1}$ as a preconditioner for the (1,1) block and $(\lambda/\|B\|^2)\widehat{M}^{-1}$ as a preconditioner for the Schur complement, where λ is the ellipticity constant of A. Thus, the theory of [3] applies, see [10].

The numerical results were obtained for the data $\Omega := (0,1)^2$, $f(x_1, x_2) := \text{sign}(x_1)\,\text{sign}(x_2)(1,1)$, $u^{(0)} := 0$, $p^{(0)} := 0$, $\varepsilon := 10^{-3}$, $\varepsilon_{\text{feas}} := 10^{-3}$, $\eta := 0.1$, $\rho^{(0)} := 1$, $\beta := 10$, $\nu := 1$. We employed Crouzeix–Raviart finite elements and a block multiplicative multigrid smoother with 3 pre– and 3 post–smothing steps. The results are depicted in Tab. 2 and they were computed in Matlab. The columns in Tab. 2 respectively denote the level, the numbers of Crouzeix–Raviart nodes, the numbers of elements, the numbers of outer iterations (before the slash in the fourth column), the numbers of inner PCG iterations throughout all the outer iterations (after the slash in the fourth column), and the sum of all the

inner PCG iterations per level. From the last column we can see that the total number of PCG iterations becomes at higher levels almost constant, which is the expected multigrid behaviour.

level l	size(u_l)	size(q_l)	outer/PCG iterations	total PCG iterations
1	56	32	**6**/1,0,1,2,4,8	**16**
2	208	128	**6**/1,0,1,2,5,13	**22**
3	800	512	**6**/1,0,1,2,5,14	**23**
4	3136	2048	**6**/1,0,1,2,6,14	**24**
5	12416	8192	**6**/1,0,1,2,6,15	**25**
6	49408	32768	**6**/1,0,1,2,6,16	**26**

Table 2. Multigrid solution to the Stokes problem

4 Coupling of Topology and Shape Optimization

The coarsely discretized optimal topology design serves as the initial guess for the shape optimization. The first step towards a fully automatic procedure is a shape identification. The second step, we are treating now, is a piecewise smooth approximation of the shape by a Bézier curve $\Gamma(p)$. Let $q_{\text{opt}} \in \mathcal{Q}$ be an optimized discretized material distribution. We solve the following least square fitting problem:

$$\min_{p \in P} \int_{\Omega} \left[q_{\text{opt}} - \chi\left(\Omega_1\left(\Gamma(p)\right)\right) \right]^2 \, dx, \tag{6}$$

where $\chi(\Omega_1)$ is the characteristic function of Ω_1.

When solving (6) numerically, one encounters a problem of intersection of the Bézier shapes with the mesh on which q_{opt} is elementwise constant. In order to avoid it we use the property that the Bézier control polygon converges linearly to the curve under the procedure that adds control nodes so that the resulting Bézier shape remains unchanged. The integration in (6) is then replaced by a sum over the elements and we deal with intersecting of the mesh and a polygon.

Note that the least square functional in (6) becomes non–differentiable whenever a shape touches the grid. Nevertheless, we compute forward finite differences, which is still acceptable for the steepest-descent optimization method that we use. The smoothness can be achieved by smoothing the characteristic function $\chi(\Omega_1)$.

We consider the benchmark problem depicted in Fig. 1 and simplified as in Fig. 4 **(a)**. Given the initial design $q_{\text{init}} := 0.5$, we start with the topology optimization. The coarse topology optimization problem involves 861 design, 1105 state variables and the optimization runs in 7 steepest descent iterations taking 2.5 seconds, when using the adjoint method for the sensitivity analysis. The second part of the computation is the shape approximation. We are looking for three Bézier curves that fit the optimized topology. There are 19 design

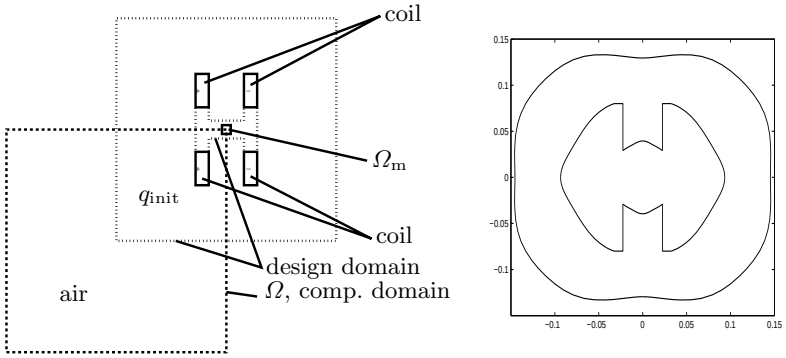

Fig. 4. Coupled topology and shape optimization: **(a)** initial topology design; **(b)** optimal shape design

parameters in total and solving the least square problem (6) runs in 8 steepest–descent iterations taking 26 seconds when using numerical differentiation. See Fig. 4 **(b)** for the resulting geometry.

References

1. Borzi, A.: Multigrid Methods for Optimality Systems, habilitation thesis, TU Graz (2003)
2. Bramble, J. H.: Multigrid Methods. John Wiley & Sons (1993)
3. Bramble, J. H., Pasciak, J. E., Vassilev, A. T.: Analysis of the inexact Uzawa algorithm for saddle point problems, SIAM J. Numer. Anal. **34** (1997) 1072–1092
4. Burger, M., Mühlhuber, W.: Numerical approximation of an SQP–type method for parameter identification, SIAM J. Numer. Anal. **40** (2002) 1775–1797
5. Dostál, Z.: Semi-monotonic inexact augmented Lagrangians for quadratic programming with equality constraints. Optimization Methods and Software **20** (2005), 715–727
6. Dreyer, T., Maar, B., Schulz, V.: Multigrid optimization in applications, J. Comp. Appl. Math. **120** (2000) 67–84
7. Hackbusch, W.: Multi–grid Methods and Applications. Springer (1985)
8. Lukáš, D., Langer, U., Lindner, E., Stainko, R., Pištora, J.: Computational shape and topology optimization with applications to 3–dimensional magnetostatics, Oberwolfach Reports **1** (2004) 601–603
9. Lukáš, D., Chalmovianský, P.: A sequential coupling of optimal topology and multilevel shape design applied to 2–dimensional nonlinear magnetostatics, Comp. Vis. Sci. (to appear)
10. Lukáš, D., Dostál, Z.: Optimal multigrid preconditioned semi–monotonic augmented Lagrangians Applied to the Stokes Problem, Num. Lin. Alg. Appl. (submitted)
11. Schöberl, J., Zulehner, W.: Symmetric indefinite preconditioners for saddle point problems with applications to PDE–constrained optimization problems, SFB Report 2006-19, University Linz (2006)

This article was processed using the LaTeX macro package with LLNCS style